Atmospheric Environment 51 (2012) 165–174

Contents lists available at SciVerse ScienceDirect

Atmospheric Environment

journal homepage: www.elsevier.com/locate/atmosenv

Sectoral and geographical contributions to summertime continental United States (CONUS) black carbon spatial distributions

Min Huang [a,*], Gregory R. Carmichael [a], Sarika Kulkarni [a,1], David G. Streets [b], Zifeng Lu [b], Qiang Zhang [c], R. Bradley Pierce [d], Yutaka Kondo [e], Jose L. Jimenez [f], Michael J. Cubison [f,2], Bruce Anderson [g], Armin Wisthaler [h]

[a] Center for Global and Regional Environmental Research, The University of Iowa, Iowa City, IA, USA
[b] Argonne National Laboratory, Argonne, IL, USA
[c] Center for Earth System Science, Tsinghua University, Beijing, China
[d] NOAA/NESDIS, Madison, WI, USA
[e] Department of Earth and Planetary Science, University of Tokyo, Tokyo, Japan
[f] CIRES and Department of Chemistry and Biochemistry, University of Colorado, Boulder, CO, USA
[g] NASA Langley Research Center, Hampton, VA, USA
[h] University of Innsbruck, Innsbruck, Austria

ARTICLE INFO

Article history:
Received 31 August 2011
Received in revised form
19 December 2011
Accepted 11 January 2012

Keywords:
Black carbon
Sectoral and geographical contributions
Warming potential

ABSTRACT

The sectoral and regional contributions from northern hemisphere anthropogenic and biomass burning emission sectors to black carbon (BC) distributions over the continental United States (CONUS) in summer 2008 are studied using the Sulfur Transport and dEposition Model (STEM). North American (NA) emissions heavily (>70% of total emissions) affect the BC levels from the surface to ~5 km, while non-NA plumes compose more than half of the BC above ~5 km. Among all sectors, NA and non-NA biomass burning, NA transportation and non-NA residential emissions are the major contributors. The sectoral contributions vary among ten regions defined by the US Environmental Protection Agency (EPA): NA anthropogenic emissions enhance northeastern US BC levels; biomass burning strongly impacts northern California and southeastern US; and the influence of extra-regional plumes is largest in the northwestern US but extends to eastern US. The mean contribution from non-NA sources to US surface BC is ~0.05 μg m^{-3}, with a maximum value of ~0.11 μg m^{-3} in the northwestern US. The non-NA contributions to column BC are higher than to surface BC, ranging from 30% to 80%, depending on region. EPA region 8 is most sensitive to extra-regional BC, partially explaining the observed increasing BC trend there during the past decades associated with the increasing Asian BC emissions. Measurements from the June 24 DC-8 flight during the ARCTAS-CARB field campaign show that BC/(organic matter + nitrate + sulfate) mass ratios fairly well represent BC's warming potential over southern California, which can be approximated by BC/(organic matter + sulfate) and BC/sulfate for plumes affected and unaffected by fires, respectively. The responses of BC/(organic matter + sulfate) and BC/sulfate to removing each emission sector are further discussed, indicating that mitigating NA transportation emissions has the highest potential for regional air quality and climate co-benefits.

© 2012 Elsevier Ltd. All rights reserved.

1. Introduction

Primary and secondary aerosols from local and distant sources influence climate (Intergovernmental Panel on Climate Change, 2007) and adversely affect human health and visibility (US Environmental Protection Agency (EPA), 2011; United Nations Environment Programme and World Meteorological Organization (UNEP and WMO), 2011). Their direct climate impact depends on the amounts of absorbing and scattering components. Black carbon (BC), generated from incomplete fossil-fuel and biomass combustion, absorbs light and has a positive direct radiative forcing (DRF). Most other aerosol components, such as sulfate (SO_4), nitrate (NO_3), and most organic carbon (OC) scatter light and have negative DRFs.

Since aerosols have short atmospheric lifetimes from hours to days (Chin, 2009), mitigating their emissions will result in rapid changes in their atmospheric concentrations and the associated

* Corresponding author. Tel.: +1 319 335 3333; fax: +1 319 335 3337.
E-mail address: mhuang1@engineering.uiowa.edu (M. Huang).
[1] Now at: Planning and Technical Support Division, California Air Resource Board, Sacramento, CA, USA.
[2] Now at: Toferk AG, Thun, Switzerland.

1352-2310/$ – see front matter © 2012 Elsevier Ltd. All rights reserved.
doi:10.1016/j.atmosenv.2012.01.021

health/climate impacts. Thus there is growing interest in developing aerosol-related policies that treat air pollution and climate change in the same framework (Ramanathan and Feng, 2008; Arneth et al., 2009). A better understanding of the sectoral contributions to the distributions of the absorbing and scattering components, and further consideration of the complication that both distant and nearby sources contribute to their health/climate impacts, will help inform these policies (Task Force of Hemispheric Transport of Air Pollution (TF HTAP), 2010; Heald et al., 2006; Brock et al., 2004; Fischer et al., 2010; Jaffe et al., 2005; VanCuren, 2003; National Research Council, 2009). Sector-based contributions to BC distributions and climate impacts have been studied using global models (*cf*, Shindell et al., 2008; Balkanski et al., 2010; Fuglestvedt et al., 2007; Koch et al., 2007; Naik et al., 2007; Unger et al., 2009). However, these estimates involve high uncertainties, due to the uncertainties in the regional and sectoral emissions, together with the uncertainties in other key model inputs, and those associated with model parameterizations and resolution (Koch et al., 2009; Textor et al., 2006). Therefore, there are needs to 1) conduct further studies over regions where observations are available to test and better constrain model estimates of BC distributions; and 2) to assess metrics that can help identify sectoral and regional contributions to climate impacts for use in screening mitigation options. For example, the ratio of BC to SO_4 over polluted Asian regions was found to be highly correlated with solar absorption efficiency (SAE = 1-single scattering albedo (SSA)), with regression slopes that differed among plume types (Ramana et al., 2010). Such useful metrics provide a measure of the relative amounts of the most important absorbing aerosol component and the major scattering component (s), but need to be evaluated over other regions, as aerosol loading, composition and optical properties may vary among regions.

In this study we estimated sectoral contributions from local and distant sources to summertime BC distributions over the continental United States (CONUS), using a regional-scale chemical transport model and a recent global BC sectoral emission inventory. We used available aircraft and surface observations during this period to evaluate the model performance. Finally, the representativeness of several metrics was also evaluated that could help prioritize BC warming impacts on climate, and their sensitivities to reductions in sectoral emissions were calculated.

2. Data and methods

2.1. Study period and observational data

This study focused on a two-week period (June 13–26, 2008). Measurements from 150 IMPROVE (Interagency Monitoring of Protected Visual Environments) sites and 28 urban (Chemical Speciation Network (CSN) and National Institute for Occupational Safety and Health (NIOSH)) over CONUS on June 14, 17, 20, 23, and 26 were used to evaluate surface BC predictions (in this paper we consistently use BC instead of elemental carbon (EC) because the emission inventories were developed for BC, and we do not consider the differences caused by measurement methods). The vertical distributions of modeled BC were evaluated using the Single Particle Soot Photometer (SP2) BC measurements on NASA DC-8 aircraft during the California (CA) phase of the Arctic Research of the Composition of the Troposphere from Aircraft and Satellites (ARCTAS-CARB) experiment. These data were collected at daytimes of June 20, 22 and 24, over southern CA, the CA-Mexico border, the Central Valley, and the eastern Pacific. Aircraft measurements of SO_4, NO_3 and organic aerosol mass (OM) sampled using the Aerosol Mass Spectrometry (AMS) instrument, together with the green band (GB) aerosol SSA measured by the Langley Aerosol Research Group (LARGE) instrument suite and acetonitrile concentrations measured by the proton-transfer-reaction mass spectrometry (PTR-MS), were also used to assess the representativeness of the BC/cooling aerosol ratios to aerosol warming potentials for different air-masses (e.g., low/high fire-impacted).

2.2. Model and input data

Model simulations were conducted using tracer and full-chemistry versions of the regional-scale Sulfur Transport and dEposition Model (STEM) version 2K3. The tracer domain used a 60 × 60 km polar stereographic grid, covering most of the northern hemisphere, and the full-chemistry domain was a subset of the tracer domain over the continental North America (NA). Further details were described in Huang et al. (2010).

The tracer model calculated aerosol distributions of BC, SO_4, primary OC, dust and sea salt (SS). Tagged CO tracers that focused on primary-emitted CO were also used to estimate the contributions of geographic source areas to the hemispheric-scale transport, including both anthropogenic (mainland US; Alaska; Canada; Greenland; Europe; Russia; China; and other Asia nations) and biomass burning (NA, North Asia/Russia, and South Asia/Africa) tracers. The tracer simulations provided aerosol boundary conditions for the full-chemistry simulations and were used to correlate regional contributions with the BC sectoral contributions estimated by the forward sensitivity simulations described in Section 2.3.

The calculations were driven by meteorological fields generated by the Advanced Research Weather Research & Forecasting Model (WRF-ARW) (D'Allura et al., 2011), and used the anthropogenic sector (industry, power, residential, transportation, and global shipping) emissions from the recent bottom-up global 1° × 1° gridded inventory developed by Q. Zhang and D. G. Streets (http://www.cgrer.uiowa.edu/arctas/emission.html) for the ARCTAS mission. The BC emissions over Asia were based largely on the NASA INTEX-B inventory (http://mic.greenresource.cn/intexb-2006), and over the CONUS were scaled from 1996 data to year of 2006 by Streets and Chin (Bond et al., 2004). The anthropogenic emissions of BC, SO_2 and OC by sector for NA and the rest of the

Table 1
Anthropogenic emissions and several emission ratios by sector. Top emission sectors for NA and non-NA regions are in bold.

Emission sectors	24-h average emissions						Ratios (dimensionless)					
	BC NA	BC non-NA	OC NA	OC non-NA	SO_2 NA	SO_2 non-NA	BC/SO_2 mass NA	BC/SO_2 mass non-NA	BC/OC NA	BC/OC non-NA	BC/(SO_2 + OC) NA	BC/(SO_2 + OC) non-NA
Anthropogenic total (molec. cm^{-2} s^{-1})	1.83E+09	5.16E+09	2.70E+09	9.86E+09	1.56E+10	2.06E+10	2.20E−02	4.71E−02	6.79E−01	5.23E−01	2.14E−02	4.32E−02
Industry (%)	18.42	24.61	8.85	11.87	27.63	33.50	1.46E−02	3.45E−02	1.41E+00	1.08E+00	1.45E−02	3.34E−02
Power (%)	1.81	1.64	1.90	0.64	**44.29**	**47.62**	8.98E−04	1.61E−03	6.44E−01	1.34E+00	8.97E−04	1.61E−03
Residential (%)	18.80	**49.22**	**64.44**	**80.12**	5.90	7.28	7.01E−02	**3.18E−01**	1.97E−01	3.22E−01	5.17E−02	1.60E−01
Transportation (%)	**59.02**	24.03	20.59	6.70	10.19	6.02	**1.27E−01**	1.88E−01	**1.94E+00**	**1.88E+00**	**1.19E−01**	**1.71E−01**
Shipping (%)	2.27	0.48	4.15	0.67	11.92	5.39	4.20E−03	4.20E−03	3.73E−01	3.73E−01	4.15E−03	4.15E−03

northern hemisphere (non-NA) are summarized in Table 1 and the spatial maps are shown in Supplemental materials (Table S1; Fig. S1). For NA, BC emissions from transportation, residential and industry sectors account for ~60%, 19% and 18% of the anthropogenic emissions, respectively, while the residential sector accounts for ~50% of the non-NA emissions, with industry and transportation adding ~24–25% each. All anthropogenic sector emissions were distributed to the first two model layers (~100 m above ground level (AGL)) with a 7:3 ratio. Point and volcano SO_2 sources were injected up to 300–500 m AGL. Diurnal cycles were included when processing the emissions but no daily and seasonal variations were considered. Daily biomass burning total CO emissions were provided by the archived Real-time Air Quality Modeling System (RAQMS) (Pierce et al., 2007) with a 12-h temporal resolution, and were then unevenly distributed from surface up to ~5–6 km AGL, with non-linear decreasing factors ranging from 0.12 to 0.013 as the model height increased. The emission factors for hydrophobic BC and OC relative to CO were ~0.016 and 0.115, respectively. During this period, frequent fires with high emissions occurred over north Asia, eastern China, northern CA and southeastern US (Fig. S1e–f).

The full-chemistry calculations also used the WRF meteorological fields and the same set of anthropogenic and biomass burning emissions as the tracer model. In addition, biogenic emissions of monoterpene and isoprene were taken from twelve-year-averaged values from the Orchidee model (Lathiere et al., 2006). Lateral boundary conditions (LBC) for thirty gaseous species and upper boundary conditions for ten gaseous species were downscaled from the RAQMS global real-time chemical analyses with a 6-h temporal resolution. The LBCs of BC, OC, dust, SS and SO_4 were from the STEM tracer results. The model treated emitted hydrophobic to hydrophilic BC and OC with ratios of 4:1 and 1:1, respectively, and both BC and OC were converted to hydrophilic with a fixed aging rate of 7.1×10^{-6} s^{-1} (Cooke and Wilson, 1996). Gas to particle conversion and water content of the inorganic aerosols were computed in four-bins (0.1–0.3 μm, 0.3–1.0 μm, 1.0–2.5 μm and 2.5–10.0 μm) by the Simulating Composition of Atmospheric Particles at Equilibrium (SCAPE) module (Kim and Seinfeld, 1995). The aerosol dry deposition rates were scaled to sulfate deposition dependent on meteorological fields and land cover, and wet scavenging was modeled as a loss rate that varied with precipitation rate, only applied to hydrophilic aerosols.

2.3. Forward sensitivity analysis

The impacts of the NA and extra-regional (interchangeable with non-NA in this paper) sector emissions on CONUS BC distributions were estimated by the base simulation and eleven forward sensitivity simulations where the sector emissions were perturbed. To estimate contributions from the NA emission sources, sector emissions of BC, OC and SO_2 from inside of the full-chemistry model domain were set to zero while the LBCs were unchanged (i.e., no changes in non-NA emissions). The contributions from extra-regional sector emissions were estimated by zeroing out sector emissions in the hemispheric tracer model and using these results as LBCs in the full-chemistry simulations where the NA emissions were not perturbed. The changes in aerosol distributions due to the perturbations in emissions had feedbacks to photolysis rates and heterogeneous chemistry, but not to the meteorological fields. In addition, we performed simulations in which the emissions from two selected sectors were perturbed by 20%, and found that the sensitivities of BC surface concentrations and column amounts to the emission perturbations were close to linear (Figs. S2–S4).

3. Results and discussions

3.1. Model base case and its evaluation

3.1.1. Base case

Fig. 1a–c presents the mean simulated BC surface concentrations, total columns and vertical profiles over the ten EPA regions (http://www.epa.gov/tp/whereyoulive/regions.htm, Fig. 1d) in the base case. The BC surface concentrations are important for assessing health impacts, and the vertical distributions and column amounts are useful for assessing climate impacts. The modeled BC surface concentrations and columns are in the ranges of ~0.05–3 μg m^{-3} and ~0.2 to ~5 mg m^{-2}, with the nation-wide averages of ~0.2 μg m^{-3} and ~1.1 mg m^{-2}, respectively. The mean surface concentration is at the higher bound of the simulated NA BC in June 2001 by six global models (TF HTAP, 2010), and the column amounts fall within the range summarized by Schuster et al. (2005). The eastern US (especially the northeastern US and the Lake Michigan areas) shows higher modeled surface concentrations and total column amounts than over most parts of the western US, except northern CA which was heavily affected by the local wildfires during this period. The four-corner region in the southwest shows the lowest values (<0.4 μg m^{-3} and <0.8 mg m^{-2}). Most of the BC mass is below ~4–5 km above sea level (ASL) (i.e., showing a ~4–5 km scale height (the altitude at which the concentration is 1/e of that at surface, which is an important input for some radiative transport models)) (Fig. 1c). Above 4–5 km, Region 10 shows the highest BC levels, reflecting the influences by extra-regional sources.

3.1.2. Evaluation at urban and remote surface sites

Comparisons between observed and modeled BC are shown in Fig. 2a–d, at 150 IMPROVE sites and 28 urban sites that had all five days of BC measurements over the CONUS domain. Table 2 summarizes the statistics of model evaluation at these sites. The observed BC at urban locations is overall ~2.5 times higher than at rural/remote sites and displays larger standard deviation (SD). Both the observed and modeled BC at IMPROVE sites show higher values over the western and eastern US than the mountain regions, and overall the model captures these gradients fairly well, with slight over-prediction over the mountain regions and negative biases over the eastern US and CA. The BC concentrations at urban locations are generally under-predicted (with a mean bias (mean modeled-observed) of −0.24 μg m^{-3}) due to the coarse model resolution and uncertainties in the fire emissions. The spatial variability reflected by SD is under-predicted at IMPROVE and urban locations by 30% and 50%, respectively.

The model performance for BC varies by individual EPA region. At IMPROVE sites, lower correlations are shown over Regions 4, and 7–10, again reflecting the uncertainties from fire emissions and extra-regional contributions. Mean biases range from −0.17 μg m^{-3} (Region 4) to 0.32 μg m^{-3} (Region 1), and root mean square errors (RMSE) are highest in Regions 1, 4 and 9. Mean fractional bias (MFB, Equation (1)) and mean fractional error (MFE, Equation (2)) at most EPA regions are below 70%.

$$\text{Mean Fractional Bias (MFB)} = \text{Mean}\,(2 \times (\text{modeled} - \text{observed})/(\text{modeled} + \text{observed})) \quad (1)$$

$$\text{Mean Fractional Error (MFE)} = \text{Mean}\,(2 \times |(\text{modeled} - \text{observed})/(\text{modeled} + \text{observed})|) \quad (2)$$

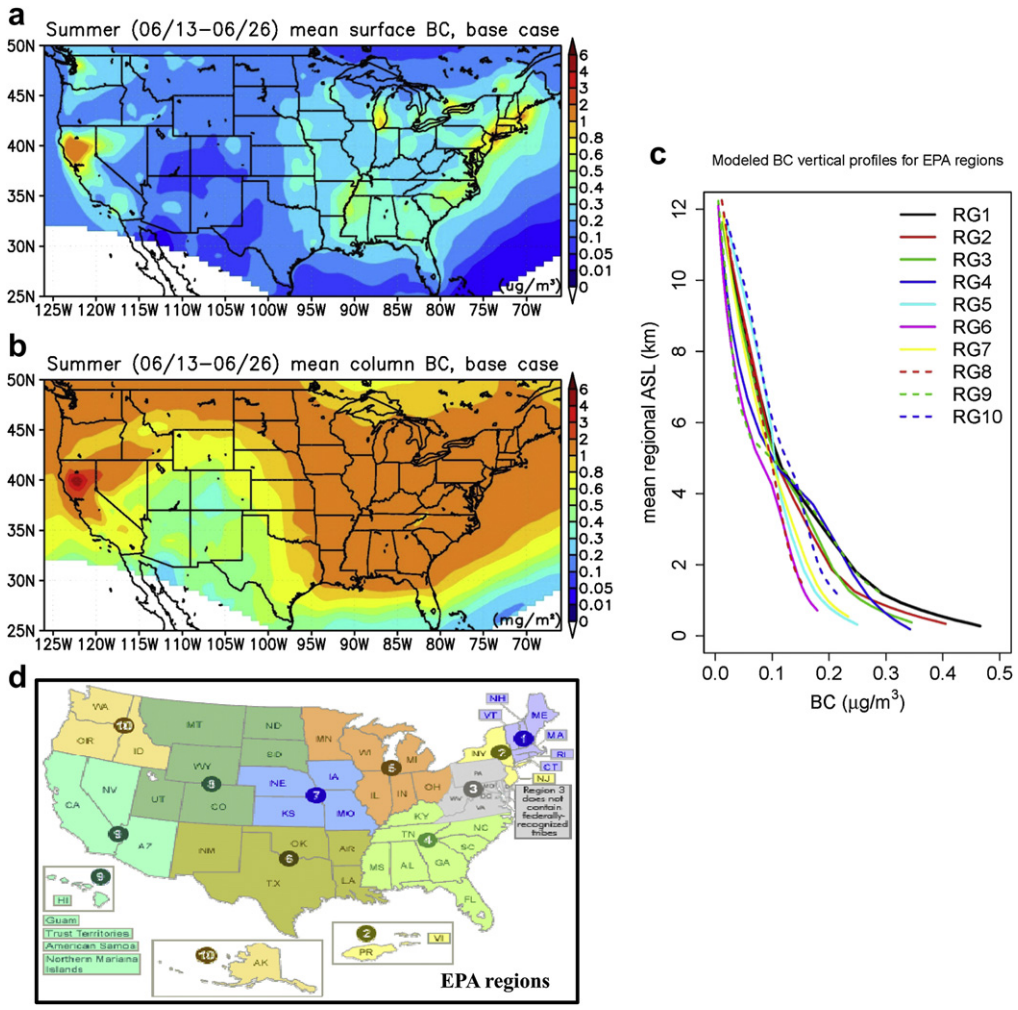

Fig. 1. Two-week (06/13–06/26) mean (a) surface BC concentrations (μg m^{-3}); (b) BC column (mg m^{-2}); (c) BC vertical distributions (μg m^{-3}) in ten EPA regions; (d) The ten EPA regions.

3.1.3. *Evaluation along DC-8 flight paths*

Predicted BC was compared to the NASA DC-8 flight observations on June 20, 22 and 24. Modeled BC was extracted at identical locations as the flight samples using spatial and temporal interpolation. The modeled and observed BC concentrations from all flights were binned vertically every 500 m and the resulting vertical distributions are presented in Fig. 2e. Observations show three major features with mean concentrations of ~0.2 μg m^{-3} below 500 m, ~0.3 μg m^{-3} at 1–1.5 km, and ~0.2 μg m^{-3} at 3.5–4 km. The multiple levels and large variability in BC concentrations indicate impacts from various sources. The model captures the vertical features fairly well, with over-predictions at the surface and >4 km. Correlations between modeled and observed BC for each of the three flights are 0.2, 0.5 and 0.1, respectively. The lower correlations for the June 20 and 24 flights reflect the model's incapability of capturing the variability over LA and the Central Valley due to its coarse horizontal resolution (relative to the speed of DC-8 at ~14 km min^{-1}). Correlations are highest for the June 22 flight that sampled over broad CA regions. Other statistical analyses for the three flights show mean biases of −0.04, 0.21 and 0.02 μg m^{-3} and the RMSE of 0.22, 0.52 and 0.34 μg m^{-3}, respectively, and the largest positive biases occur at the northern CA fire locations.

Compared to global model performance summarized by Koch et al. (2009), the STEM performance is reasonably good (i.e., seventeen global models over-predicted BC at NA surface and along flight tracks in several field campaigns over tropical/mid-latitude regions, with the mean modeled/observed BC ratios of 1.6 and 7.9, respectively, while the mean modeled/observed BC burden over NA from these models was 0.42.)

3.2. *Sector contributions to CONUS BC distributions*

3.2.1. *Contributions to surface/column distributions and vertical profiles*

The stacked mean contributions from eleven emission sectors to CONUS surface and column BC, averaged over the ten EPA regions are shown in Fig. 3a and b, respectively. The numbers below each stacked bar indicate the base case results for the corresponding region. The surface concentrations range from 0.15 μg m^{-3} (Region 8) to 0.47 μg m^{-3} (Region 1) and column amounts range from 0.76 mg m^{-2} (Region 6) to 1.45 mg m^{-2} (Region 1). The sum of contributions from all sectors for each region shows a 5%–15% loss due to the averaging processes and the exchanges between regions and with Mexico and Canada (included in the full-chemistry domain but not belonging to the EPA regions). Overall, NA transportation and extra-regional residential sectors are the major anthropogenic contributors to surface and column BC. The contributions from NA emissions to column BC are lower than those to surface BC, indicating that the impacts of transported plumes increase with altitude. The sectoral contributions vary among

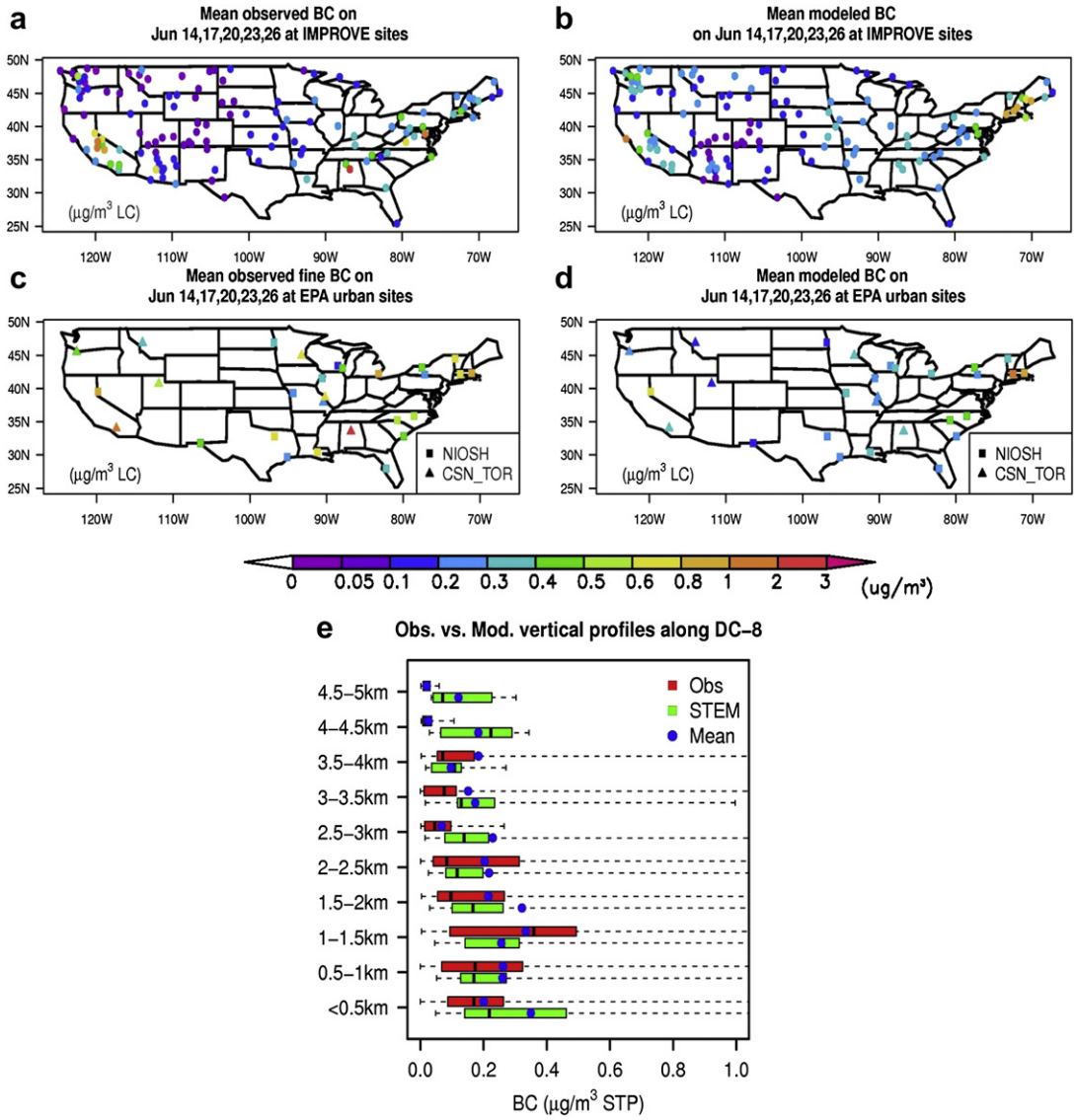

Fig. 2. Mean (a) observed and (b) modeled BC (μg m^{-3}) on June 14, 17, 20, 23, 26 at the IMPROVE sites; Mean (c) observed and (d) modeled BC (μg m^{-3}) on June 14, 17, 20, 23, 26 at the EPA urban sites; (e) Observed and modeled BC (μg m^{-3}, at standard temperature and pressure) vertical profiles shown as boxplots along June 20, 22, 24 DC-8 flight tracks.

Table 2
Statistical evaluation of modeled summertime BC at surface sites, summarized by EPA regions.[a,b]

	RG1	RG2	RG3	RG4	RG5	RG6	RG7	RG8	RG9	RG10	All IMPROVE sites	All urban sites
Observation, mean ± σ	0.27 ± 0.10	0.30	0.47 ± 0.27	0.46 ± 0.53	0.18 ± 0.10	0.15 ± 0.08	0.16 ± 0.05	0.08 ± 0.04	0.37 ± 0.33	0.12 ± 0.12	0.24 ± 0.27	0.60 ± 0.38
Bias, mean/σ	0.32/0.20	−0.03	−0.15/−0.19	−0.17/−0.43	0.01/−0.02	0.02/−0.01	0.10/0.02	0.07/0.01	−0.12/−0.12	0.14/−0.03	0.02/−0.08	−0.24/−0.19
Mean Error	0.32	0.03	0.16	0.19	0.04	0.04	0.10	0.07	0.24	0.15	0.15	0.28
Correlation *r*	0.88	NA	0.70	0.41	0.82	0.77	0.50	0.24	0.13	0.67	0.30	0.27
Mean Fractional Bias	0.66	−0.12	−0.30	−0.18	0.10	0.15	0.46	0.55	−0.25	0.91	0.25	−0.42
Mean Fractional Error	0.67	0.12	0.31	0.28	0.24	0.22	0.47	0.57	0.64	0.94	0.54	0.53
Root Mean Square Error	0.39	0.03	0.25	0.50	0.05	0.05	0.11	0.09	0.38	0.17	0.27	0.44
Number of sites	13	1	8	13	11	11	12	31	32	18	150	28

[a] Results are in μg m^{-3} except correlation *r* and the number of sites.
[b] The statistics by EPA region refer to the IMPROVE sites; there are too few numbers of urban sites with observations in each EPA region for statistics.

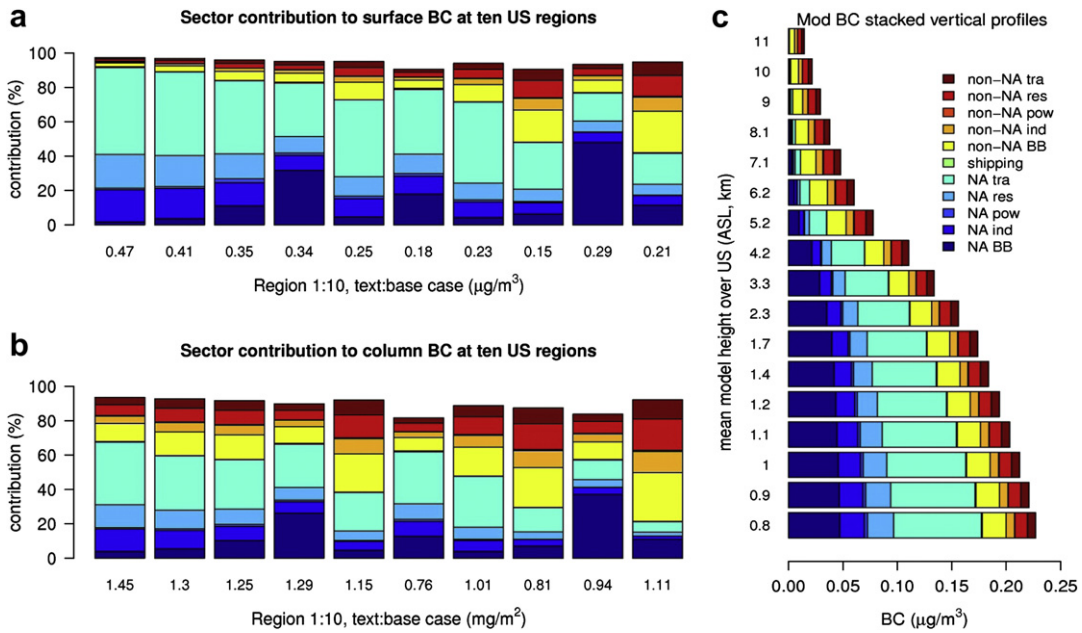

Fig. 3. Stack plots of contributions from eleven sectors to US (a) surface BC (μg m^{-3}); (b) column BC (mg m^{-2}); (c) BC vertical profiles (μg m^{-3}) during 06/13–06/26, 2008.

regions. Regions 8 and 10 receive the largest contributions from extra-regions (~40–60% at surface and >60% for column), while the rest of the regions are dominated by NA emissions. NA biomass burning strongly impact Regions 4 and 9 (~30–50% at surface and for column), and extra-regional biomass burning BC accounts more than half of the extra-regional BC in Regions 8 and 10.

Fig. 3c shows the sectoral contributions to the BC vertical distribution averaged over the CONUS domain. The NA sectors (mainly biomass burning and transportation) are the major contributors below ~5 km. The non-NA emissions dominate the BC distribution above ~5 km, but also contribute ~25% to the mean surface concentration.

To further estimate the importance of extra-regional BC, we calculated the spatial correlations between modeled surface BC concentrations (NA anthropogenic and NA anthropogenic + extra-regional total) and US anthropogenic emissions (Table 3), and the temporal correlation between modeled surface BC and column BC amounts (Fig. 4a). The modeled anthropogenic NA concentrations show correlations with anthropogenic emissions >0.65, mostly >0.8. After we added the modeled extra-regional BC contributions into the correlation calculations, the values dropped (except Region 5) by 0.02–0.33, due to the modifications of BC distributions by the transported plumes. The largest changes (−0.33) occur at Region 8 (mountain regions), indicating that this region is most sensitive to the transported plumes, because of its complex topography and lower local emissions. Region 10 follows Region 8 and shows a decrease in correlation of 0.09. Fig. 4a depicts the temporal correlations between modeled surface and column BC over CONUS during the period. The eastern Pacific, coastal Oregon, Washington, Utah, Colorado and urban regions in EPA Region 9 (such as LA and Phoenix) show the lowest correlations (<±0.1), indicating that the boundary layer and free troposphere are influenced by different emissions sources/processes. There are broad regions with high correlations, which may be generally influenced dominantly by either NA or non-NA sources.

We also compared the extra-regional estimates of BC obtained through the sector-based analysis with the estimates using the regional CO tracers. Shown in Fig. 4b are the ratios of the extra-regional tracer CO (%) to the extra-regional BC contributions (%) at surface and their spatial correlations during the study period for the ten EPA regions. The large-scale features of the estimates are similar, reflected by the high spatial correlations between the two (>0.7). The highest correlations are in Regions 5, 8–10 (>0.94), and the lowest are in Regions 2, 3 and 7 (~0.7–0.8). The extra-regional contributions based on tracer CO are higher than those for BC (ratios >1), mainly due to the differences in their lifetimes and emission characteristics over NA and extra-regions. The ratios increase as the travel distances increase (e.g., Regions 1–4 > Regions 8–10).

3.2.2. Evaluation of the extra-regional BC contributions

VanCuren (2003) conducted composition analysis of Asian aerosols for March–October, 1989–1999 at multiple IMPROVE sites in western US. He found that a mixture of dust and combustion products dominated the Asian aerosols with typical concentration around 5 μg m^{-3} and mass median diameter between 2 and 3 μm. BC accounted for ~4% of the fine particles (~0.1 μg m^{-3}). Model simulations by Park et al. (2003) reported that the contributions from non-US sources to US BC in 1998 were 0.06 μg m^{-3} over both western and eastern US (0.04 and 0.02 μg m^{-3} from natural and anthropogenic sources, respectively). Six global models estimated the non-NA source contributions to the annual mean NA surface BC concentrations in 2001 (TF HTAP, 2010), showing the range of 0.8–45.5% with the median value of 20.9%. Our study generated a mean non-NA contribution (biomass burning + anthropogenic) to CONUS surface

Table 3
Correlation *r* between emissions and BC concentrations, summarized by EPA regions.

	RG1	RG2	RG3	RG4	RG5	RG6	RG7	RG8	RG9	RG10
r (anthropogenic BC emissions vs. modeled NA anthropogenic BC)	0.95	0.92	0.93	0.82	0.67	0.8	0.85	0.83	0.88	0.88
r (anthropogenic BC emissions vs. modeled NA anthropogenic BC + non-NA BC)	0.95	0.92	0.93	0.74	0.70	0.76	0.83	0.50	0.84	0.79
Degradation in *r* by extra-regional plumes	~0	~0	~0	−0.08	0.03	−0.04	−0.02	−0.33	−0.04	−0.09

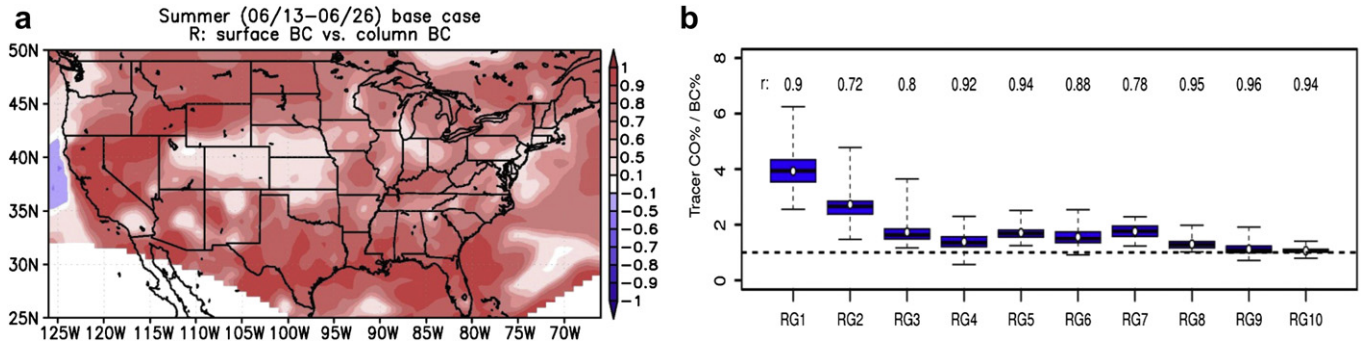

Fig. 4. (a) Temporal correlation *r* between surface and column BC during 06/13–06/26, 2008; (b) Comparison between tracer extra-regional CO% and extra-regional BC% calculated by the forward sensitivity simulations for ten EPA regions.

BC of ~0.05 μg m^{-3} (~20% of total), with the maximum of ~0.11 μg m^{-3} in Region 10. These values are close to these previous studies, but with a higher spatial variability than Park et al. (2003).

Murphy et al. (2011) analyzed the observed BC at IMPROVE sites during 1990–2004 and indicated that BC concentrations decreased over most regions in summertime except the mountain regions due to the wildfires. However, our results for a low fire-impacted summer period over the mountain regions show that the trend of extra-regional emissions (Lu et al., 2011) may also play a role in this trend. This is similar as Jaffe and Ray (2007) and Jaffe et al. (2008)'s suggestion that the summertime western US fires together with regional emissions and global background are responsible for the increase in summertime ozone over the western US.

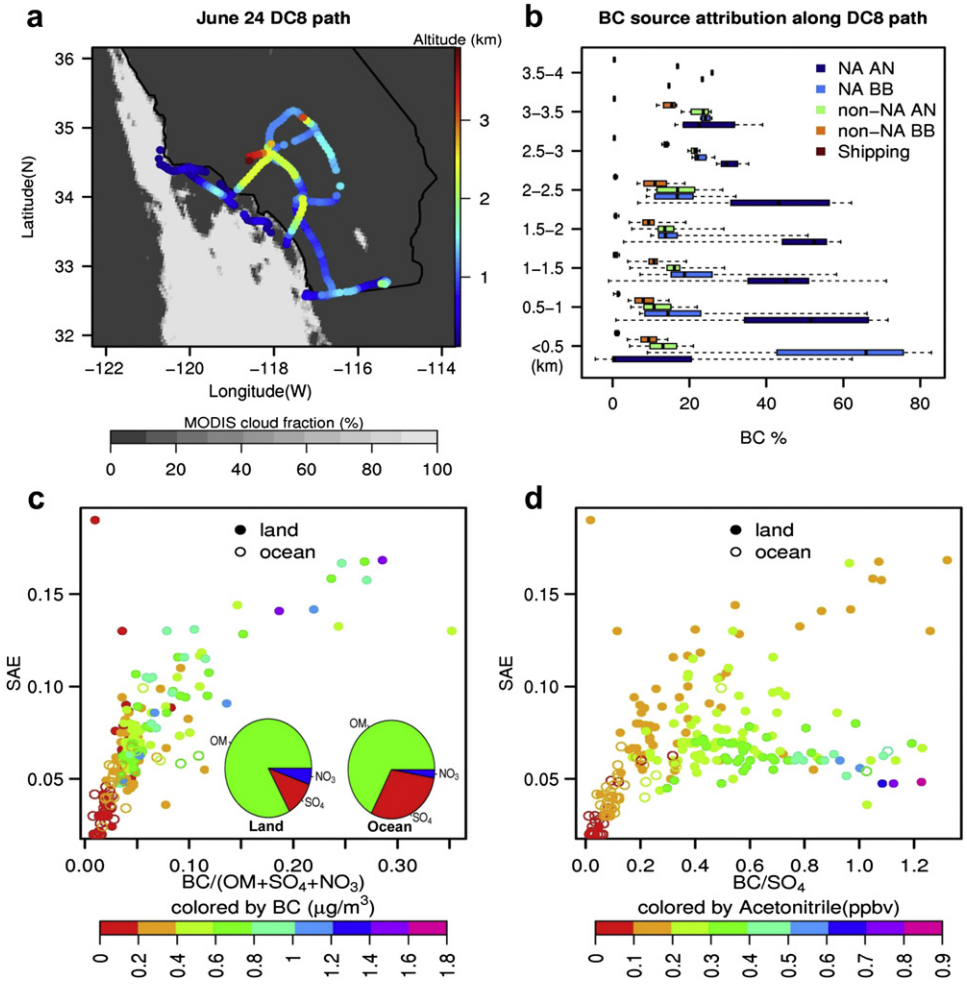

Fig. 5. (a) The June 24 DC-8 flight path (where aerosols, acetonitrile and green band SSA measurements were made), colored by flight altitude (ASL, km), overlaid on MODIS cloud fraction at 18:45 UTC (11:45 am PDT); (b) BC source attribution along the flight, shown every 500 m in boxplots, AN and BB stand for anthropogenic and biomass burning, respectively; (c) Scatter plot of SAE against BC/(OM + SO_4 + NO_3), colored by observed BC. Inner panel are pie plots of cooling aerosol compositions along the path in (a) for terrestrial and oceanic samples; (d) Scatter plot of SAE against BC/SO_4, colored by observed acetonitrile. (MODIS: Moderate Resolution Imaging Spectroradiometer).

Table 4
Correlations between BC/cooling aerosols and SAE[a] along the June 24 DC-8 flight.

Ratios	BC/(OM + SO_4 + NO_3)	BC/(OM + SO_4)	BC/OM	BC/SO_4
High fire-impacted[b]	0.76	0.78	0.78	−0.04
Low fire-impacted[b]	0.78	0.78	0.76	0.77

[a] SAE = 1-single scattering albedo, green band (~532 nm).
[b] High-fire: acetonitrile >0.2 ppb; Low-fire impacted: acetonitrile <=0.2 ppb. Median of measured acetonitrile was ~0.23 ppb.

3.3. Using metrics to prioritize climate impacts of sector emissions

3.3.1. Evaluate metrics to prioritize climate impacts

A previous study over Asia found that BC/SO_4 ratios were highly correlated with GB SAE (i.e., 550 nm) (Ramana et al., 2010). The SAE indicates aerosols' warming potential: Empirical values for warming and cooling aerosol plumes are >0.15 and <0.05, respectively, and for values between 0.05 and 0.15, the aerosols' climate impact depends on the surface and cloud properties, atmosphere vertical profile, location and season (Bond and Bergstrom, 2006). We used the June 24 DC-8 observations to evaluate the correlation between the BC and cooling aerosol ratios and the GB SAE (i.e., 532 nm) over CA. The sampling locations where aerosol, acetonitrile and SAE measurements were made are mostly below 3 km, over southern CA and the CA-Mexico border cloud-free regions (Fig. 5a). The calculated BC source contributions at these locations are shown as boxplots every 500 m in Fig. 5b. The sampled regions are mostly affected by NA anthropogenic (AN) and biomass burning (BB) emissions, but are also influenced by extra-regional sources, with their contributions increasing with altitudes. Fig. 5c–d show the scatterplots between the BC and cooling aerosol ratios (i.e., BC/(OM + NO_3 + SO_4), and BC/SO_4) and the GB SAE, colored by measured BC and acetonitrile, respectively. Measured SAE ranges from ~0 to 0.2, and the samples with BC >0.2 μg m^{-3} show SAE >0.05. Fire-impacted samples (defined in this study as those with acetonitrile >0.2 ppb, as the median of the measured acetonitrile that we used is ~0.23 ppb at these locations) have SAE values in the 0.05–0.1 range, while the anthropogenic plumes indicate higher warming potential with SAE values up to ~0.2. The oceanic samples are mostly unaffected by fires and have lower BC concentrations and SAE. The ratios of BC/(OM + SO_4 + NO_3) are highly correlated with SAE for both terrestrial and oceanic samples (0.74 over land and 0.72 over ocean). The BC/SO_4 ratio shows negative correlation with SAE for the high fire-impacted airmasses, but positive correlation for the low fire-impacted plumes. Table 4 summarizes the correlations of SAE with several ratios. These results indicate that BC/(OM + NO_3 + SO_4) can fairly well represent their net warming potential over the LA region. It can be approximated by BC/(OM + SO_4) and BC/OM (as OM accounts for >~70% of the sum of OM + NO_3 + SO_4 aerosols, Fig. 5c inner panels). For the low-fire impacted plumes, the representativeness of BC/(OM + SO_4) is slightly better than BC/OM. BC/SO_4 is also a good metric for plumes unaffected by fires.

3.3.2. BC/(SO_4 + OM) and BC/SO_4 sensitivity to sector emissions

Using the ratios of BC/(SO_4 + OM) and BC/SO_4 as metrics to represent the impacts of aerosol mixture on DRF for fire-impacted and non-fire-impacted scenarios, respectively, we calculated their responses to removing sector emissions for the ten EPA regions. To calculate the BC/SO_4 ratios in the base and non-anthropogenic sector emission cases, we subtracted the contributions from NA and non-NA biomass burning from each sensitivity case, and ignored any non-linear impacts on SO_4. The modeled BC and SO_4 were scaled with observed/modeled BC and SO_4 at the IMPROVE sites for each region, and modeled OC was converted to OM using 1.8× observed OC/modeled OC (1.8 came from "Key to Monitoring-Modeling-Emissions Mapping", 2008, http://vista.cira.colostate.edu/docs/AirData/Methods/). This scaling approach assumes that: 1) the biases in each sector are the same as those in the base case in each region; 2) biases determined by the five-day measurements represent the two-week period; 3) biases determined by observations at sparse sites in each EPA region represented the entire corresponding region Scaling factors are given in Table S2.

The ratios in the base case and their percent changes relative to the base case ratios after removing various emission sectors are summarized in Tables 5 and 6 for BC/(SO_4 + OM) and BC/SO_4, respectively. Both ratios indicate that power and shipping sectors have net cooling impacts (positive changes) and transportation sectors are net warming, with the NA power and transportation sectors the largest cooling and warming sectors, respectively. As the transportation sector contributes most to the surface and column BC among the NA anthropogenic emission sectors (Section 3.2), controlling emissions from this sector can efficiently reduce BC concentrations and the aerosol warming potentials over the CONUS.

Previous studies have discussed the impacts of sector emissions on radiative forcing and climate change. They found that controlling BC + OM from fossil-fuel combustion can slow warming (Jacobson, 2002), while biomass burning had short-term cooling effects (Jacobson, 2004; Naik et al., 2007). Among the anthropogenic emission sectors, transportation emissions showed positive forcing while industry and power sector emissions contributed negative forcing (Shindell et al., 2008). Residential emissions resulted in weak cooling effects over CONUS except over northwestern US (Koch et al., 2007). The metrics we analyzed agreed well with previous findings for transportation, power, and biomass burning sectors. BC/(OM + SO_4) and BC/SO_4 showed discrepancies in representing residential and industry sectors, and they were consistent with Koch et al. (2007)'s results for residential and industry sectors, respectively.

Table 5
Base case BC/(SO_4 + OM) ratios and the responses in ratios to removing emission sectors, by EPA regions.

Cases		RG1	RG2	RG3	RG4	RG5	RG6	RG7	RG8	RG9	RG10
Base (×10^{-2})		5.36	6.31	5.51	5.55	5.29	3.29	4.64	3.54	4.23	4.77
Changes in %	no NA biomass burning	3.91	4.85	7.54	16.66	7.10	15.88	8.34	8.22	50.35	8.07
	no NA industry	−5.74	−4.74	−2.86	−0.15	−1.85	2.89	−1.37	−3.60	−3.95	−4.79
	no NA power	25.87	27.51	26.10	15.68	13.12	14.38	10.29	2.98	0.38	0.20
	no NA residential	16.15	12.87	4.83	0.40	4.98	−0.51	4.30	1.11	1.41	−1.07
	no NA transportation	−44.16	−42.09	−36.59	−26.61	−39.62	−32.12	−42.33	−24.34	−14.02	−16.25
	no shipping	1.68	0.65	0.44	1.98	0.42	3.28	0.83	1.46	1.17	1.75
	no non-NA biomass burning	1.48	1.61	1.62	0.97	10.91	2.53	16.81	21.52	2.24	14.48
	no non-NA industry	0.26	−0.06	−0.60	−0.67	−0.10	−0.22	0.40	0.07	−0.47	1.13
	no non-NA power	1.48	1.49	1.49	1.49	4.00	1.90	4.71	8.95	2.74	13.55
	no non-NA residential	−0.28	−0.61	−1.21	−1.36	−0.89	−0.93	−0.01	−2.23	−1.66	−4.22
	no non-NA transportation	−0.65	−1.00	−1.61	−1.65	−2.70	−1.42	−2.54	−5.04	−2.07	−6.12

Table 6
Base case BC/SO_4 ratios and the responses in ratios to removing emission sectors, by EPA regions. The NA biomass burning and non-NA biomass burning contributions were subtracted from each case before the calculations.

Cases		RG1	RG2	RG3	RG4	RG5	RG6	RG7	RG8	RG9	RG10
Base		0.11	0.13	0.10	0.11	0.13	0.07	0.13	0.10	0.17	0.10
Changes in %	no NA industry	5.83	7.70	6.53	12.83	13.53	22.61	13.58	0.36	−1.17	−6.94
	no NA power	73.68	87.59	86.32	72.43	53.71	49.98	44.35	12.80	4.53	0.80
	no NA residential	−10.26	−12.49	−12.29	−11.46	−10.59	−12.62	−9.20	−7.04	−8.99	−8.89
	no NA transportation	−47.97	−47.36	−45.34	−43.52	−47.44	−41.62	−50.50	−33.55	−31.82	−26.62
	no shipping	3.34	1.35	0.96	6.27	1.18	8.65	2.56	5.38	12.98	5.94
	no non-NA industry	1.10	0.78	−0.03	−0.01	3.98	0.94	6.03	13.25	12.51	17.69
	no non-NA power	3.13	3.33	3.45	4.79	13.17	5.12	17.13	43.46	33.77	65.79
	no non-NA residential	−0.92	−1.54	−2.86	−3.86	−4.27	−2.82	−4.04	−9.25	−5.27	−13.62
	no non-NA transportation	−0.63	−1.05	−1.96	−2.62	−2.89	−1.81	−2.59	−5.81	−3.23	−8.63

4. Conclusions and future work

We calculated the contributions of various anthropogenic and biomass burning sector emissions to BC surface/vertical distributions and column amounts in summer 2008 over ten EPA regions. Over 80% of the surface BC concentrations were dominated by NA emissions except for Regions 8 and 10, and the non-NA emissions contributed to 30–80% of column BC depending on region. NA fires were important during this period in northern CA and southeastern US, and NA transportation sector was the largest anthropogenic contributor in general. The mean non-NA contribution to surface BC was ~0.05 μg m^{-3}, with a maximum value of ~0.11 μg m^{-3} in Region 10. Residential, transportation and biomass burning were the major non-NA contributors.

The representativeness of BC to cooling aerosol mass ratios to their warming potential (SAE) were evaluated using the June 24 DC-8 flight observations during the ARCTAS-CARB field campaign. BC/OM, BC/(OM + SO_4) and BC/(OM + SO_4 + NO_3) correlated well with SAE and BC/SO_4 only correlated well with SAE for the low-fire impacted plumes. Forward sensitivity calculations suggested that reducing emissions from NA transportation sector is likely to have highest co-benefits for air quality and climate change. Further research is needed to evaluate the utility of these (and other) metrics over broad geographical regions, and to extend the analysis to include sector-based NO_x emissions perturbations.

There were still uncertainties associated with the sectoral/regional contribution estimates. Uncertainties were mainly resulted from the emission inventory (±208% uncertainty over China, with much lower uncertainty for the power sector than the others (Zhang et al., 2009)), and from the uncertainty in estimating transport processes in the complex topography in Regions 8–10. Three-dimensional observations are useful to constrain BC distributions, improve emission estimates, and to improve estimates of sector-based NA and extra-regional contributions. Combining these observations with modeling studies using an appropriate resolution will help reduce these uncertainties.

Acknowledgments

We thank two anonymous reviewers for their constructive comments. We thank the ARCTAS science team. We thank CGRER members A. D'Allura, B. Adhikary and C. Wei who contributed to building the STEM forecast modeling system for ARCTAS. The Iowa group was supported by NASA awards (NNX08AH56G and NNX11AI52G) and an EPA award (RD-83503701-0). M. J. Cubison and J. L. Jimenez were supported by a NASA award (NNX08AD39G). Acetonitrile measurements were supported by the Austrian Research Promotion Agency (FFG-ALR) and the Tiroler Zukunftstiftung and were carried out with the help/support of T. Mikoviny, M. Graus, A. Hansel and T. D. Maerk.

Appendix. Supplementary material

Supplementary material associated with this article can be found, in the online version, at doi:10.1016/j.atmosenv.2012.01.021.

References

Arneth, A., Unger, N., Kulmala, M., Andreae, M., 2009. Clean air, heat the planet? Science 326, 672–676. doi:10.1126/science.1181568.

Balkanski, Y., Myhre, G., Gauss, M., Rädel, G., Highwood, E.J., Shine, K.P., 2010. Direct radiative effect of aerosols emitted by transport: from road, shipping and aviation. Atmospheric Chemistry and Physics 10, 4477–4489. doi:10.5194/acp-10-4477-2010.

Bond, T.C., Bergstrom, R.W., 2006. Light absorption by carbonaceous particles: an investigative review. Aerosol Science and Technology 40, 27–67. doi:10.1080/02786820500421521.

Bond, T.C., Streets, D.G., Yarber, K.F., Nelson, S.M., Woo, J.-H., Klimont, Z., 2004. A technology-based global inventory of black and organic carbon emissions from combustion. Journal of Geophysical Research 109, D14203. doi:10.1029/2003JD003697.

Brock, C.A., Hudson, P.K., Lovejoy, E.R., Sullivan, A., Nowak, J.B., Huey, L.G., Cooper, O.R., Cziczo, D.J., de Gouw, J., Fehsenfeld, F.C., Holloway, J.S., Hubler, G., Lafleur, B.G., Murphy, D.M., Neuman, J.A., Nicks, D.K., Orsini, D.A., Parrish, D.D., Ryerson, T.B., Tanner, D.J., Warneke, C., Weber, R.J., Wilson, J.C., 2004. Particle characteristics following cloud-modified transport from Asia to North America. Journal of Geophysical Research 109, D23S26. doi:10.1029/2003JD004198.

Chin, M., 2009. Atmospheric Aerosol Properties and Climate Impacts. http://downloads.climatescience.gov/sap/sap2-3/sap2-3-final-report-all.pdf.

Cooke, W.F., Wilson, J.J.N., 1996. A global black carbon aerosol model. Journal of Geophysical Research 101 (D14), 19395–19409. doi:10.1029/96JD00671.

D'Allura, A., Kulkarni, S., Carmichael, G.R., Finardi, S., Adhikary, B., Wei, C., Streets, D.G., Zhang, Q., Pierce, R.B., Al-Saadi, J.A., Diskin, G., Wennberg, P., 2011. Meteorological and air quality forecasting using the WRF-STEM model during the 2008 ARCTAS field campaign. Atmospheric Environment 45, 6901–6910. doi:10.1016/j.atmosenv.2011.02.073.

Fischer, E.V., Jaffe, D.A., Marley, M., Gaffney, J., Marchany-Rivera, A., 2010. Optical properties of aged Asian aerosols observed over the U.S. Pacific Northwest. Journal of Geophysical Research 115, D20209. doi:10.1029/2010JD013943.

Fuglestvedt, J., Berntsen, T., Myhre, G., Rypdal, K., Skeie, R.B., 2007. Climate forcing from the transport sectors. Proceedings of the National Academy of Sciences of the United States of America 105, 454–458. doi:10.1073/pnas.0702958104.

Heald, C.L., Jacob, D.J., Park, R.J., Alexander, B., Fairlie, T.D., Yantosca, R.M., Chu, D.A., 2006. Transpacific transport of Asian anthropogenic aerosols and its impact on surface air quality in the United States. Journal of Geophysical Research 111, D14310. doi:10.1029/2005JD006847.

Huang, M., Carmichael, G.R., Adhikary, B., Spak, S.N., Kulkarni, S., Cheng, Y.F., Wei, C., Tang, Y., Parrish, D.D., Oltmans, S.J., D'Allura, A., Kaduwela, A., Cai, C., Weinheimer, A.J., Wong, M., Pierce, R.B., Al-Saadi, J.A., Streets, D.G., Zhang, Q., 2010. Impacts of transported background ozone on California air quality during the ARCTAS-CARB period – a multi-scale modeling study. Atmospheric Chemistry and Physics 10, 6947–6968. doi:10.5194/acp-10-6947-2010.

Task Force on Hemispheric Transport of Air Pollution (TF HTAP), 2010. Final Assessment Report, Part A: Ozone and Particulate Matter. http://www.htap.org/activities/2010_Final_Report/HTAP%202010%20Part%20A%20110407.pdf.

Intergovernmental Panel on Climate Change, 2007. Contribution of Working Group I to the Fourth Assessment Report of the Intergovernmental Panel on Climate Change. The Physical Science Basis. Cambridge University Press, Cambridge, United Kingdom and New York, NY, USA.

Jaffe, D., Tamura, S., Harris, J., 2005. Seasonal cycle, composition and sources of background fine particles along the west coast of the U.S. Atmospheric Environment 39, 297–306. doi:10.1016/j.atmosenv.2004.09.016.

Jaffe, D., Ray, J., 2007. Increase in surface ozone at rural sites in the Western U.S. Atmospheric Environment 41, 5452–5463. doi:10.1016/j.atmosenv.2007.02.034.

Jaffe, D.A., Hafner, W., Chand, D., Westerling, A., Spracklen, D., 2008. Influence of fires on O_3 concentrations in the Western U.S. Environmental Science and Technology 42 (16), 5885–5891. doi:10.1021/es800084k.

Jacobson, M.Z., 2002. Control of fossil-fuel particulate black carbon plus organic matter, possibly the most effective method of slowing global warming. Journal of Geophysical Research 107 (D19), 4410. doi:10.1029/ 2001JD001376.

Jacobson, M.Z., 2004. The short-term cooling but long-term global warming due to biomass burning. Journal of Climate 17, 2909–2926.

Koch, D., Bond, T.C., Streets, D., Unger, N., van der Werf, G.R., 2007. Global impacts of aerosols from particular source regions and sectors. Journal of Geophysical Research 112, D02205. doi:10.1029/2005JD007024.

Koch, D., Schulz, M., Kinne, S., McNaughton, C., Spackman, J.R., Balkanski, Y., Bauer, S., Berntsen, T., Bond, T.C., Boucher, O., Chin, M., Clarke, A., De Luca, N., Dentener, F., Diehl, T., Dubovik, O., Easter, R., Fahey, D.W., Feichter, J., Fillmore, D., Freitag, S., Ghan, S., Ginoux, P., Gong, S., Horowitz, L., Iversen, T., Kirkevåg, A., Klimont, Z., Kondo, Y., Krol, M., Liu, X., Miller, R., Montanaro, V., Moteki, N., Myhre, G., Penner, J.E., Perlwitz, J., Pitari, G., Reddy, S., Sahu, L., Sakamoto, H., Schuster, G., Schwarz, J.P., Seland, Ø., Stier, P., Takegawa, N., Takemura, T., Textor, C., van Aardenne, J.A., Zhao, Y., 2009. Evaluation of black carbon estimations in global aerosol models. Atmospheric Chemistry and Physics 9, 9001–9026. doi:10.5194/acp-9-9001-2009.

Kim, Y.P., Seinfeld, J.H., 1995. Atmospheric gas–aerosol equilibrium: III. Thermodynamics of crustal elements Ca^{2+}, K^{+}, and Mg^{2+}. Aerosol Science and Technology 22 (1), 93–110.

Lathiere, J., Hauglustaine, D.A., Friend, A.D., De Noblet-Ducoudre, N., Viovy, N., Folberth, G.A., 2006. Impact of climate variability and land use changes on global biogenic volatile organic compound emissions. Atmospheric Chemistry and Physics 6, 2129–2146. doi:10.5194/acp-6-2129-2006.

Lu, Z., Zhang, Q., Streets, D.G., 2011. Sulfur dioxide and primary carbonaceous aerosol emissions in China and India, 1996–2010. Atmospheric Chemistry and Physics 11, 9839–9864. doi:10.5194/acp-11-9839-2011.

Murphy, D.M., Chow, J.C., Leibensperger, E.M., Malm, W.C., Pitchford, M., Schichtel, B.A., Watson, J.G., White, W.H., 2011. Decreases in elemental carbon and fine particle mass in the United States. Atmospheric Chemistry and Physics 11, 4679–4686. doi:10.5194/acp-11-4679-2011.

Naik, V., Mauzerall, D.L., Horowitz, L.W., Schwarzkopf, M.D., Ramaswamy, V., Oppenheimer, M., 2007. On the sensitivity of radiative forcing from biomass burning aerosols and ozone to emission location. Geophysical Research Letter 34, L03818. doi:10.1029/2006GL028149.

National Research Council, 2009. Global Sources of Local Pollution-An Assessment of Long-Range Transport of Key Air Pollutants to and from the United States. The National Academies Press. http://www.nap.edu/openbook.php?record_id=12743&page=67, 67–96 pp.

Park, R.J., Jacob, D.J., Chin, M., Martin, R.V., 2003. Sources of carbonaceous aerosols over the United States and implications for natural visibility. Journal of Geophysical Research 108 (D12), 4355. doi:10.1029/2002JD003190.

Pierce, R.B., Schaack, T., Al-Saadi, J.A., Fairlie, T.D., Kittaka, C., Lingenfelser, G., Natarajan, M., Olson, J., Soja, A., Zapotocny, T., Lenzen, A., Stobie, J., Johnson, D., Avery, M.A., Sachse, G.W., Thompson, A., Cohen, R., Dibb, J.E., Crawford, J., Rault, D., Martin, R., Szykman, J., Fishman, J., 2007. Chemical data assimilation estimates of continental U.S. ozone and nitrogen budgets during the Intercontinental Chemical Transport Experiment–North America. Journal of Geophysical Research 112, D12S21. doi:10.1029/2006JD007722.

Ramana, M., Ramanathan, V., Feng, Y., Yoon, S.-C., Kim, S.-W., Carmichael, G.R., Schauer, J.J., 2010. Warming influenced by black carbon to sulfate ratio and black carbon source. Nature Geoscience 3 (8), 542–545. doi:10.1038/ngeo918.

Ramanathan, V., Feng, Y., 2008. On avoiding dangerous anthropogenic interference with the climate system: formidable challenges. Proceedings of the National Academy of Sciences 105, 14245–14250. doi:10.1073/pnas.0803838105.

Schuster, G.L., Dubovik, O., Holben, B.N., Clothiaux, E.E., 2005. Inferring black carbon content and specific absorption from Aerosol Robotic Network (AERONET) aerosol retrievals. Journal of Geophysical Research 110, D10S17. doi:10.1029/2004JD004548.

Shindell, D., Lamarque, J.-F., Unger, N., Koch, D., Faluvegi, G., Bauer, S., Ammann, M., Cofala, J., Teich, H., 2008. Climate forcing and air quality change due to regional emissions reductions by economic sector. Atmospheric Chemistry and Physics 8, 7101–7113. doi:10.5194/acp-8-7101-2008.

Textor, C., Schulz, M., Guibert, S., Kinne, S., Balkanski, Y., Bauer, S., Berntsen, T., Berglen, T., Boucher, O., Chin, M., Dentener, F., Diehl, T., Easter, R., Feichter, H., Fillmore, D., Ghan, S., Ginoux, P., Gong, S., Grini, A., Hendricks, J., Horowitz, L., Huang, P., Isaksen, I., Iversen, I., Kloster, S., Koch, D., Kirkevåg, A., Kristjansson, J.E., Krol, M., Lauer, A., Lamarque, J.F., Liu, X., Montanaro, V., Myhre, G., Penner, J., Pitari, G., Reddy, S., Seland, Ø., Stier, P., Takemura, T., Tie, X., 2006. Analysis and quantification of the diversities of aerosol life cycles within AeroCom. Atmospheric Chemistry and Physics 6, 1777–1813. doi:10.5194/acp-6-1777-2006.

United Nations Environment Programme and World Meteorological Organization (UNEP and WMO), 2011. Integrated Assessment of Black Carbon and Tropospheric Ozone: Summary for Decision Makers. http://www.unep.org/dewa/Portals/67/pdf/Black_Carbon.pdf.

US Environmental Protection Agency, 2011. Report to Congress on Black Carbon. http://yosemite.epa.gov/sab/sabproduct.nsf/fedrgstr_activites/05011472499C2FB28525774A0074DADE/$File/BC+RTC+External+Peer+Review+Draft-opt.pdf.

Unger, N., Bond, T.C., Wang, J.S., Koch, D.M., Menon, S., Shindell, D.T., Bauer, S., 2009. Attribution of climate forcing to economic sectors. Proceedings of the National Academy of Sciences 107, 3382–3387. doi:10.1073/pnas.0906548107.

VanCuren, R.A., 2003. Asian aerosols in North America: extracting the chemical composition and mass concentration of the Asian continental aerosol plume from long-term aerosol records in the western United States. Journal of Geophysical Research 108 (D20), 4623. doi:10.1029/2003JD003459.

Zhang, Q., Streets, D.G., Carmichael, G.R., He, K.B., Huo, H., Kannari, A., Klimont, Z., Park, I.S., Reddy, S., Fu, J.S., Chen, D., Duan, L., Lei, Y., Wang, L.T., Yao, Z.L., 2009. Asian emissions in 2006 for the NASA INTEX-B mission. Atmospheric Chemistry and Physics 9, 5131–5153. doi:10.5194/acp-9-5131-2009.